

A 0.9-2.6 GHz Broadband RF Front-end For Direct Conversion Transceivers

Munenari Kawashima, Hitoshi Hayashi, Tadao Nakagawa,
Kenjiro Nishikawa, and Katsuhiko Araki

NTT Network Innovation Laboratories, NTT Corporation, Yokosuka-Shi, Kanagawa, 239-0847, Japan

ABSTRACT — A broadband radio frequency (RF) front-end for direct conversion transceivers has been developed. The RF front-end consists of a broadband low-noise variable gain amplifier (LNVGA) and broadband quadrature mixers. The LNVGA achieves high linear characteristics by using a feedback circuit and broadband characteristics by not using reactance elements such as inductors or capacitors. The mixer achieves broadband characteristics through the incorporation of an in-phase power divider and a 45-degree power divider. The in-phase power divider achieves broadband characteristics through the addition of a compensation capacitor. The 45-degree power divider achieves broadband phase characteristics through the addition of capacity to increase the resonance point. From 0.9 GHz to 2.6 GHz, the LNVGA shows a noise figure of less than 2.1 dB and a gain of 28 ± 1.6 dB. The mixer for a demodulator shows an amplitude error of less than 1.6 dB and a phase error of less than 3 degrees. The mixer for a modulator shows an image ratio of less than -30 dBc.

I. INTRODUCTION

Software-defined radios are effective tools for use in the terminals used in mobile communications [1], [2]. The terminals need to have broadband characteristics, since they must deal with various radio frequencies. It is difficult to manufacture broadband terminals with the superheterodyne architecture used in most mobile terminals, though, because such terminals have image-rejection filters and intermediate frequency (IF) channel filters that cannot be programmed. Thus, the direct conversion architecture is a more suitable tool for broadband terminals. Terminals using this architecture do not require image-rejection filters or IF-channel filters, because they convert radio frequency (RF) signals directly to baseband signals. Therefore, the direct conversion architecture has a potential to achieve broadband characteristics. However, terminal components such as the amplifier and power dividers should also have broadband characteristics.

In this paper, we report on a broadband RF front-end for direct conversion transceivers that uses a low-noise variable gain amplifier (LNVGA) and power dividers which achieve broadband characteristics. We show that they are suitable for broadening the frequency band, and

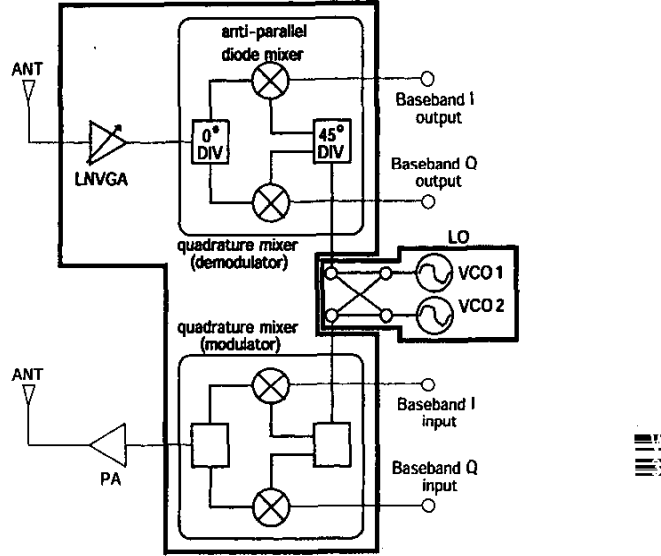


Fig. 1. Block diagram of the RF front-end for direct conversion transceivers.

also show the measurement results we obtained from fabricated monolithic microwave integrated circuits (MMIC).

II. RF FRONT-END

Figure 1 shows a block diagram of our RF front-end, which consists of an LNVGA and quadrature mixers. The target frequencies are the 900-MHz band (e.g. cellular phones), the 1.9-GHz band (e.g. cordless phones), and the 2.4-GHz band (e.g. wireless local area networks). The same quadrature mixers are used for both a demodulator and a modulator. Thus, a local oscillator can be shared between the receiver and the transmitter. The RF front-end connects the multiband local oscillator [3].

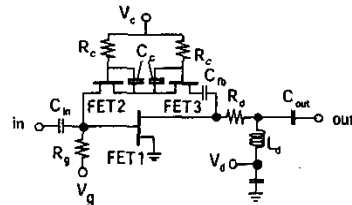


Fig. 2. Circuit configuration of the LNVGA.

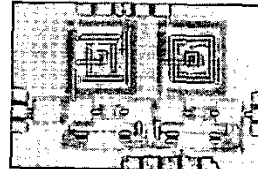


Fig. 3. Chip photograph of the LNVGA.

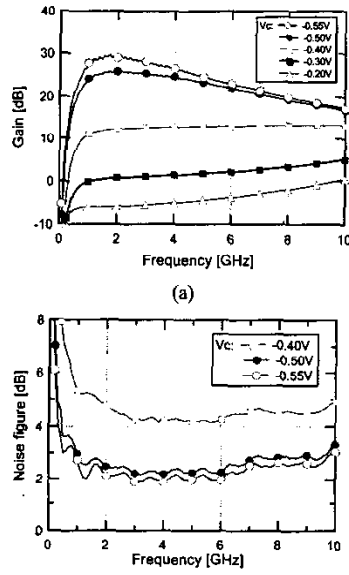


Fig. 4. LNVGA performance: (a) gain, (b) noise figures.

III. LOW-NOISE VARIABLE GAIN AMPLIFIER

The variable gain amplifier is used in the IF stage of terminals with the superheterodyne architecture to control the gain. In terminals with the direct conversion architecture, however, a gain-control mechanism in the RF stage is needed because there is no IF stage. We have therefore developed a low-noise variable gain amplifier in the RF stage.

Figure 2 shows the circuit configuration of the LNVGA.

The amplifier uses variable feedback resistance that consists of two anti-series HEMTs and two capacitors. This feedback circuit has high linearity. Therefore, the amplifier can obtain high linearity at the gain control. To achieve broadband characteristics, no matching circuits using reactance elements were used.

The LNVGA was fabricated using UMS 0.15- μ m GaAs pHEMT technology. Figure 3 shows a photograph of the chip, which employs two-stage amplifiers. The chip size is 1.3 mm \times 2.0 mm. The measured gain and noise figures are shown in Fig. 4. From 900 MHz to 2.5 GHz, the maximum gain is more than 26 dB, the noise figure at maximum gain is less than 3.1 dB, and the variable gain control range is more than 30 dB. From 1.9 GHz to 6.3 GHz, the noise figure at maximum gain is less than 2.3 dB. The power consumption is 50 mA with a 2.0-V supply. This amplifier thus features broadband, low noise, and high linear performance.

III. QUADRATURE MIXER

Our quadrature mixer consists of anti-parallel diode mixers, a in-phase power divider, a 45-degree power divider and differential amplifiers (Fig. 5). Despite the fact that direct-conversion architecture has the disadvantages of second-order distortion and DC-offset, these disadvantages can be eliminated by using the anti-parallel diode mixer [4],[5]. This mixer connects in parallel diodes that have the same characteristics in reverse, so basically no even-order signals are output. Consequently, the second-order distortion and DC-offset, equivalent to zero-order distortion, are suppressed. Moreover, the anti-parallel diode mixer is an even-harmonic mixer which uses LO signals whose frequency is one-half that of the RF signals. To generate in-phase and quadrature signals, we used a 45-degree phase shifter in the LO power divider.

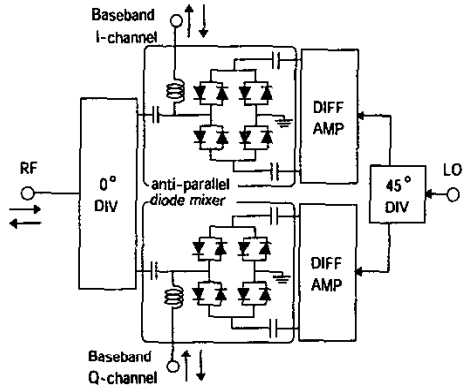


Fig. 5. Circuit configuration of the quadrature mixer.

A. In-phase Power Divider

Figure 6 shows the circuit configuration of our in-phase power divider, which includes a compensation capacitor (C_4) where the frequency band is broadened. The reflection characteristic S_{11} has at most two minimum values, because the circuits are fifth-order high pass filters. The reflection characteristic S_{22} and the isolation characteristic S_{32} also have at most two minimum values, because the resonant point increases as a result of adding the compensation capacitor, and the divider thus satisfies the matching conditions at two frequencies. This enables the divider to exhibit broadband characteristics.

Figure 7 shows our S-parameter simulation results. Lumped passive elements were set so that the matching conditions are satisfied at 0.8 GHz and 1.2 GHz. S_{11} , S_{22} and S_{32} each have two minimum values, which enables the divider's broadband characteristics.

B. 45-degree Power Divider

Figure 8 shows the circuit configuration of our 45-degree power divider, which includes a compensation capacitor (C_1) and a compensation resistor (R_2) where the frequency band is broadened. The 45-degree power divider consists of a band-pass filter and a high-pass filter using RC-networks. The phase $\theta_b(\omega)$ of the band-pass filter, which consists of C_1 , C_3 , and R_1 , is given by

$$\theta_b(\omega) = \tan^{-1} \left\{ -\frac{b}{a} \times \omega + \frac{c}{a \times \omega} \right\}, \quad (1)$$

$$a = 1 + (Z_s + R_1) / Z_1 + C_3 / C_1, \quad b = (Z_s + R_1) \times C_1,$$

$$c = 1 / (Z_1 \times C_1).$$

The phase $\theta_h(\omega)$ of the high-pass filter, which consists of C_2 , R_2 , and R_3 , is given by

$$\theta_h(\omega) = \tan^{-1} \left\{ \frac{e}{d \times \omega} \right\}, \quad (2)$$

$$d = 1 + (Z_s + R_2) \times (1 / Z_1 + 1 / R_3), \quad e = (1 / Z_1 + 1 / R_3) / C_2.$$

Equation (1) shows that the phase characteristic of the band-pass filter has one inflection point as a function frequency. Equation (2) shows that the phase characteristic of the high-pass filter decreases monotonically as a function frequency. Therefore, because the phase difference has at most two extreme values, the divider achieves broadband characteristics.

Figure 9 shows the S-parameter simulation results. Lumped passive elements were set so that the amplitude difference is 0 dB and the phase difference is 45 degrees at 1.0 GHz. The phase difference has two extreme values. Therefore, the divider exhibits broadband characteristics.

C. Fabrication and Measurement Results

The proposed broadband quadrature mixer was designed

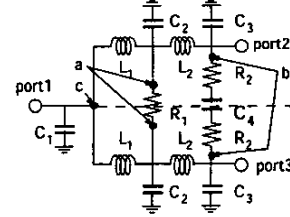


Fig. 6. Circuit configuration of the in-phase power divider.

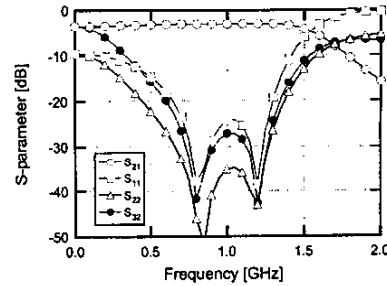


Fig. 7. Simulated S-parameter of the in-phase power divider.

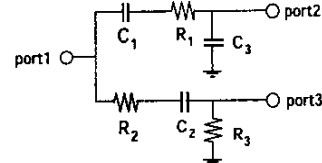


Fig. 8. Circuit configuration of the 45-degree power divider.

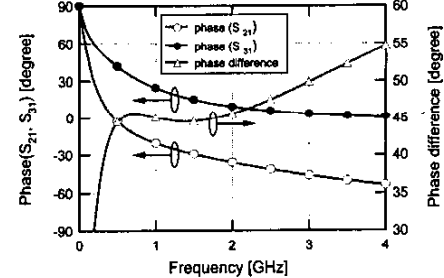


Fig. 9. Simulated S-parameter of the 45-degree power divider.

and fabricated using a 0.3- μ m GaAs MESFET process with $f_t = 20$ GHz and $f_{max} = 70$ GHz. A photograph of the chip is shown in Fig. 10. The chip size is 1.8 mm x 2.3 mm.

The measured amplitude balance and phase difference of output signals in the demodulation characteristic is shown in Fig. 11. The frequency of RF signals (f_{RF}) was varied from 0.8 GHz to 3.0 GHz. The frequency of the baseband signal was not zero (144 kHz), because the

amplitude and the phase difference were measured with an oscilloscope. The frequency of LO signals was $(f_{RF} - 144 \text{ kHz}) / 2$, and the RF power level was set to -20 dBm. The LO power level was set to +5 dBm. When the RF signal frequency was between 900 MHz and 2.6 GHz, the amplitude imbalance and the phase difference were less than 1.6 dB and 3 degrees, respectively. As a result, the mixer covered all the target frequencies.

Modulation functions were tested using the SSB method in which the image ratio (IR) corresponds to amplitude and phase errors [6]. Figure 12 shows the frequency characteristic of the RF output power. A 144-kHz baseband signal with a phase difference of 90 degrees was input, and the frequency was converted directly into an RF signal of frequency f_{RF} according to the LO signal of frequency $f_p = (f_{RF} - 144 \text{ kHz}) / 2$. The input level of the baseband signal is 500 mVp-p. The input level of the LO signal is +5 dBm in the frequency of 0.7 - 2.3 GHz, and +10 dBm in the frequency of 2.4 GHz or more. When the RF signal frequency was between 0.9 GHz and 2.7 GHz, the IR was less than -30 dBc and the leakage signal level at frequency $2f_p$ was less than -40 dBm. This IR indicates the phase error is less than 3.6 degrees with the assumption of a 0-dB amplitude error.

V. CONCLUSION

We have developed an RF front-end for direct conversion transceivers that comprises a low-noise variable gain amplifier and a quadrature mixer. The amplifier achieves high linear characteristics by using a variable gain controlled circuit and broadband characteristics by not using reactance elements. From 900 MHz to 2.5 GHz, the maximum gain is more than 28 ± 1.6 dB, the noise figure at maximum gain is less than 3.1 dB, and the variable gain control range is more than 30 dB. The mixer achieves broadband characteristics through the use of broadband power dividers. When the RF frequency is between 900 MHz and 2.6 GHz, the demodulator mixer shows an amplitude error of less than 1.6 dB and a phase error of less than 3 degrees. When the RF frequency is between 900 MHz and 2.7 GHz, the modulator mixer shows an IR of less than -30 dBc.

REFERENCES

- [1] A. Abidi, "Direct-conversion radio transceivers for digital communications," *IEEE J. Solid-State Circuits*, vol. SC-30, no. 12, pp. 1394-1410, February 1999.
- [2] H. Tsurumi and Y. Suzuki, "Broadband RF stage architecture for software-defined radio in handheld terminal applications," *IEEE Commun. Mag.*, pp. 90-95, February 1999.
- [3] T. Nakagawa, M. Kawashima, H. Hayashi, and K. Araki, "A 0.9-2.5 GHz wideband direct conversion receiver for multi-band applications," *2001 IEEE GaAs IC Symp. Dig.*, pp. 37-40, October 2001.
- [4] D. Neuf, "Fundamental, harmonic and sampling MESFET mixer circuits," *Microwave Journal*, pp. 76-58, December 1995.
- [5] K. Itoh, M. Shimozawa, N. Suematsu, and O. Ishida, "Even harmonic type direct conversion receiver ICs for mobile handsets," *1999 IEEE RFIC Symp. Dig.*, pp. 53-56, June 1999.
- [6] J. W. Archer, J. Granlund, and R. E. Mauzy, "A Broad-band UHF mixer exhibiting high image rejection over a multidecade baseband frequency range," *IEEE J. Solid-State Circuits*, vol. SC-16, no. 4, pp. 385-392, August 1981.

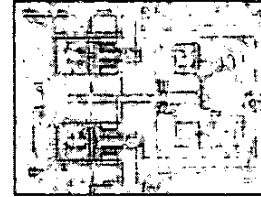


Fig. 10. Chip photograph of the quadrature mixer.

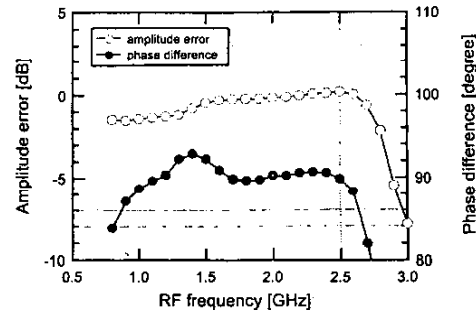


Fig. 11. Measured amplitude balance and phase difference of the quadrature mixer for the demodulator.

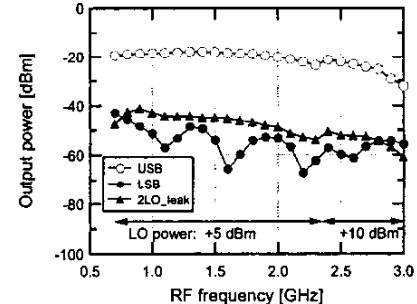


Fig. 12. Measured output signals and leakage signals of the quadrature mixer for the modulator.